
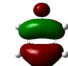
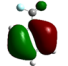
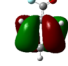
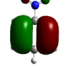
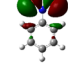


# Substituent Effect in the First Excited Singlet State of Monosubstituted Benzenes

Jan Cz. Dobrowolski,<sup>\*,†</sup> Piotr F. J. Lipiński,<sup>‡</sup> and Grażyna Karpińska<sup>†</sup><sup>†</sup>Department for Medicines Biotechnology and Bioinformatics, National Medicines Institute, 30/34 Chełmska Street, 00-725 Warsaw, Poland<sup>‡</sup>Department of Neuropeptides, Mossakowski Medical Research Centre PAS, 5 Pawińskiego Street, 02-106 Warsaw, Poland

## S Supporting Information

**ABSTRACT:** sEDA, pEDA, and cSAR descriptors of the substituent effect were determined for >30 monosubstituted benzenes in the first excited singlet  $S_1$  state at the LC- $\omega$ B97XD/aug-cc-pVTZ level. It was found that in the  $S_1$  state, the  $\sigma$ - and  $\pi$ -valence electrons are a bit less and a bit more affected, respectively, than in the  $S_0$  state, but basically, the effect in both states remains the same. In the  $S_0$  and  $S_1$  states, the  $d(C-X)$  distances to the substituent's first atom and the ring perimeter correlate with the sEDA and pEDA in the appropriate states, respectively. The energies and the gap of the frontier orbitals in the two states are linearly correlated and for the HOMO( $S_1$ ), LUMO( $S_1$ ), and HOMO( $S_1$ )–LUMO( $S_1$ ) gap correlate also with the pEDA( $S_1$ ) and cSAR( $S_1$ ) descriptors. In all studied correlations, three similar groups of substituents can be distinguished, for which correlations (i) are very good, (ii) deviate slightly, and (iii) deviate significantly. Comparison of the shape of the HOMO( $S_0$ ) and HOMO( $S_1$ ) orbitals shows that for case (i) HOMO orbitals exhibit almost perfect antisymmetry against the benzene plane, for case (ii) the antisymmetry of HOMO in one of the states is either perturbed or changed, and for case (iii) one HOMO state has  $\sigma$ -character.

HOMO orbital in the monosubstituted benzene		Similarity of the Substituent Effects
Ground Singlet	First Excited Singlet	
	Cl 	great
	CFO 	visible discrepancies
	NO <sub>2</sub> 	great difference

## 1. INTRODUCTION

The fluorescence of organic molecules from the first excited to the ground singlet state has a multitude of applications, including in organic light-emitting diodes,<sup>1,2</sup> molecular photo-switches,<sup>3,4</sup> biosensors,<sup>5,6</sup> chemosensors,<sup>7,8</sup> microscopy,<sup>9–11</sup> imaging,<sup>12,13</sup> image-guided surgery,<sup>14,15</sup> phototherapy of cancer,<sup>16,17</sup> etc. Excited states are of interest also for their photoreactivity, which offers conditions for performing unique syntheses.<sup>18,19</sup> Molecular design in these fields aims to tune the fluorescence properties (e.g., the fluorescence maximum, intensity, bandwidth, or radiation lifetime), while conserving other properties (e.g., what is required to be a medicine/ligand, a sensor, or a valuable technical material). The most basic but still powerful modification leading to the desired properties is the introduction of a certain functional group of known electron donor and acceptor properties. However, the rational design of such modifications should be based on precise descriptors of the substituent effects elicited by the functional group in the excited state.

The most important and widely used electronic substituent effect descriptors<sup>20</sup> (including the Hammett constants) have been derived using ground-state reactions and processes (e.g., dissociation of benzoic acids, NMR chemical shifts, etc.). As the geometry and electronic structure of molecules in excited states can sometimes be significantly different from those in the ground state,<sup>21</sup> the question of whether these classical ground-

state descriptors could be used to accurately model the excited-state properties arises. In the past, they often were. Successful description with the classical Hammett constants<sup>20</sup> was achieved for quantities as different as excited-state  $pK_a^*$  values of aromatic acids and bases,<sup>22–25</sup> absorption or fluorescence maxima,<sup>26–32</sup> fluorescence quantum yields,<sup>33</sup> transition-state free energies for the fluorescence quenching reaction,<sup>34</sup> excited-state lifetimes,<sup>35–41</sup> and rate constants for the nonradiative deactivation<sup>36</sup> (see page S3 of the Supporting Information for a more detailed description). Another ground-state descriptor (derived computationally), pEDA(I), served to model modern, excited-state photodevices.<sup>42–45</sup>

There were also examples in which the ground-state descriptors were perceived to be inaccurate, and researchers introduced novel constants designed for the excited states. The first descriptor constructed to directly express the substituent effect in the first singlet excited state was probably Baldry's  $\sigma_{ex}$  constant, based on  $pK_a^*$  values of para- and meta-substituted phenols in the first excited singlet state.<sup>46</sup> The descriptor proved to be better in correlating some other excited-state reactivity data rather than the ground-state descriptors, so the author concluded that there was a benefit in using the constants

Received: March 6, 2018

Revised: April 26, 2018

Published: April 26, 2018

designed especially for the excited state. However, a subsequent study<sup>47</sup> showed that yields and quantum yields for the photoaddition of methanol to nine 1-phenylbutadienes correlated more strongly with the ground-state substituent constants than with the excited-state ones. An analogous approach based on phenols and benzoic acids was adopted by Shim et al.<sup>48,49</sup> for  $pK_a^*$  correlations of several substituted benzene derivatives, which appeared to be much better than those built using the classical  $\sigma$ ,  $\sigma^+$ , and  $\sigma^-$  Hammett constants.<sup>20</sup>

The Cao, Chen, and Yin  $\sigma_{CC}^{ex}$  constant<sup>50</sup> was determined on the basis of the  $\lambda_{max}$  of the  $K$ -band<sup>51</sup> in the ultraviolet (UV) spectra of substituted benzenes and para-disubstituted stilbenes. It correlated neither with the  $\sigma_p$  Hammett constant<sup>20</sup> nor with any other substituent constants, yet significant correlations with the UV absorption energies of several types of substituted compounds have been demonstrated.<sup>50,52</sup> Further studies attempted to better predict the UV absorption energy of a series of para-disubstituted phenylethenyl benzenes.<sup>53</sup> The  $\sigma_{CC}^{ex}$  constant has also been shown to be useful for studying the influence of the substituent on reduction potentials of substituted aniline derivatives.<sup>54</sup> The adequacy of the  $\sigma_{CC}^{ex}$  constant for this problem has been explained by the similarity of an electron in the reduction process to the electron distribution after absorbing a photon. Indeed, the use of  $\sigma_{CC}^{ex}$  constants remarkably improved the correlations for substituted benzenamines, acetophenones, and naphthalenes. The  $\sigma_{CC(m)}^{ex}$  constant has recently been applied to study the UV spectra of >200 disubstituted stilbenes and benzenes.<sup>55</sup> The main objections to the construction of the  $\sigma_{CC}^{ex}$  constant come from the Franck–Condon principle. However, the principle refers to the overlap between two vibrational wave functions in the ground and excited states.<sup>56</sup> In the first approximation, it says that the electronic transition is vertical and occurs without a change in the ground-state geometry that would significantly determine the UV absorption energy. Therefore, does the  $\sigma_{CC}^{ex}$  constant really describe first of all the excited-state properties?

The need to construct substituent effect descriptors of the first excited  $\pi$  singlet state<sup>57</sup> was investigated by Sadlej-Sosnowska and Kijak by adopting Sadlej-Sosnowska's substituent active region (SAR) approach (see Methods).<sup>58–61</sup> They analyzed the computationally derived potentials and charges on atoms of the functional groups in both para-substituted benzoic acids and nitrosobenzenes and  $C_{ipso}$  atoms. It appeared that these quantities in both the ground state and the excited state are equally well modeled with the classical  $\sigma_p$  Hammett constant.<sup>20</sup> Also, the  $\Delta cSAR$  descriptors estimating the amount of charge transferred between the active regions of the two functional groups ( $\Delta$  and  $c$  stand for difference and charge, respectively) if calculated for the singlet excited state or the ground state are strongly correlated with  $\sigma_p$ . The  $cSAR$  descriptor is the sum of charges of the  $C_{ipso}$  and substituent atoms.<sup>57,58</sup>

In this work, we examine the problem of the singlet excited-state substituent effects from the point of view of yet another class of descriptors: sEDA and pEDA (where s, p, and EDA stand for  $\sigma$ ,  $\pi$ , and electron donor–acceptor, respectively).<sup>62–65</sup> The sEDA and pEDA descriptors are calculated as the difference in a population of  $\sigma$ - and  $\pi$ -valence orbitals, respectively, on the C atoms of the substituted and unsubstituted benzene rings.<sup>62</sup> The descriptors quantify the amount of electrons donated to or withdrawn from the valence  $\sigma$ - and  $\pi$ -electron system. The effect on  $\sigma$ - and  $\pi$ -electron

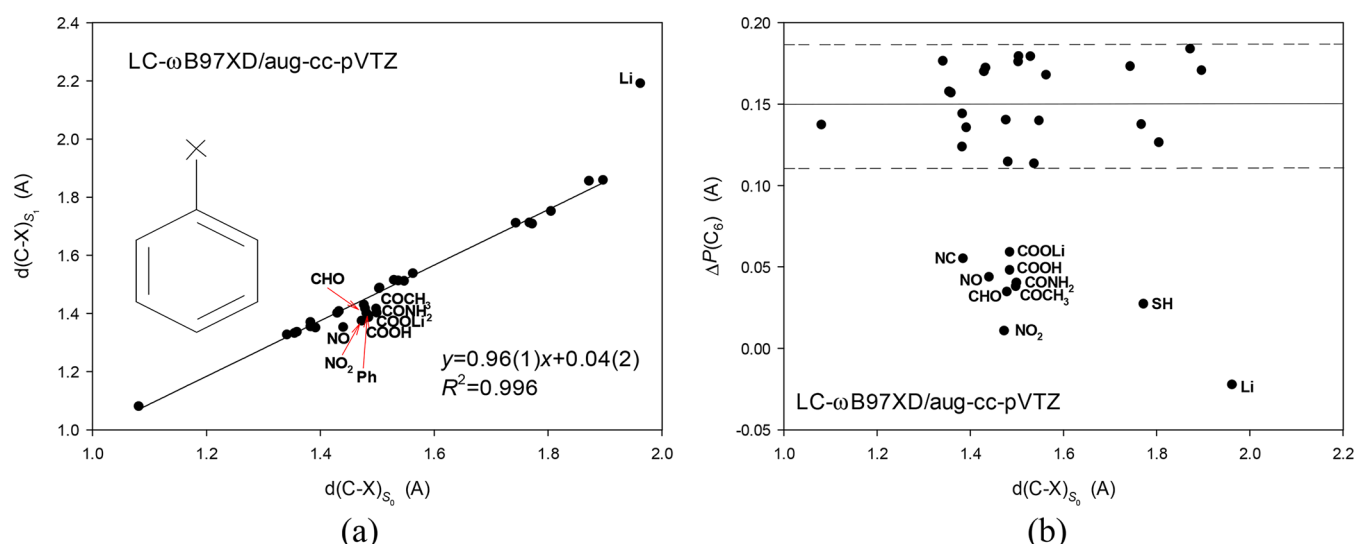
structure is expressed by the sEDA and pEDA descriptors, respectively. The sEDA descriptors are a kind of group-electronegativity parameters, whereas the pEDA descriptors specify some resonance characteristics. The sEDA and pEDA descriptors appeared to be useful and so far have been applied in a few dozen studies, including a few papers modeling the properties of molecules in excited states.<sup>42–45</sup> However, can they correctly describe the substituent effect in excited states? To answer this question, we constructed the sEDA and pEDA descriptors for >30 monosubstituted benzenes in the  $S_1$  excited state. Like their analogues in the ground state, they quantify the amount of electrons donated to or withdrawn from the  $\sigma$ - and  $\pi$ -electron systems of molecules in the  $S_1$  state. Additionally, for the same set of molecules in the excited state, we calculated the cSAR substituent effect descriptor of Sadlej-Sosnowska. This descriptor directly characterizes the substituent rather than the substituted core. A comparison of the sEDA, pEDA, and cSAR descriptors in ground and excited singlet states explains the success of the classical substituent constants in analyses of the properties of molecules in their excited states. On the other hand, the same comparison reveals the existence of several substituents for which such an analysis fails regardless the descriptor used.

## 2. METHODS

**2.1. Calculations.** The calculations were performed by using the Gaussian 09 revision D.01 suite of programs.<sup>66</sup> The geometries of >30 benzene monoderivatives in the ground and first singlet excited states were optimized, following the (restricted, closed-shell) DFT<sup>67</sup> and TD-DFT<sup>68</sup> approaches using B3LYP,<sup>69–71</sup> CAM-B3LYP,<sup>72</sup> and LC- $\omega$ B97XD<sup>73</sup> functionals and the aug-cc-pVTZ basis set.<sup>74,75</sup> The former functional was used with and without the D3 Grimme's correction for dispersion forces;<sup>76</sup> CAM-B3LYP was used only with the correction, while LC- $\omega$ B97XD, which has the dispersion correction included by definition,<sup>73</sup> was used without the additional term. The harmonic frequencies of the optimized geometries in the ground and excited states were determined to be all positive to ascertain that the structures are true minima.

The charge and population analysis was conducted according to the NBO method<sup>77</sup> as implemented in the Gaussian 09 revision D.01 suite of programs.<sup>66</sup> The sEDA, pEDA, and cSAR descriptors for the ground and first singlet excited states were determined as for the ground states.<sup>57,62</sup> The sEDA and pEDA values are calculated as a difference in  $\sigma$ - and  $\pi$ -electron valence electron populations of the ring C atoms in the monosubstituted benzenes, respectively. The cSAR descriptor is the sum of the charges in the so-called substituent active region, that is the atoms of the substituent and the  $C_{ipso}$  atom of the ring.

The basic idea of the SAR approach is to calculate a substituted molecule and to select the atoms most responsible for the substituent effect and then use their properties to construct the descriptor. Analogously to the classical Hammett constant, the benzoic acids were taken to construct the SAR descriptor in the ground<sup>58–61</sup> and excited states. All atoms of the substituent and the  $C_{ipso}$  atom have been demonstrated to constitute the substituent active region, while the sum of their charges or the sum of their potentials was singled out as the probing property.<sup>58–61</sup> Here, partial charges used for determining the cSAR descriptors were calculated using the NBO method,<sup>77</sup> as well.



**Figure 1.** Comparison of some geometrical parameters in the ground and excited states of the monosubstituted benzenes: (a)  $C_{\text{ipso}}\text{--X}$  distance and (b) difference in ring perimeters  $\Delta P(C_6) = P(C_6)(S_1) - P(C_6)(S_0)$  with respect to the  $C_{\text{ipso}}\text{--X}$  distance.

Correlation analysis was performed using the SigmaPlot 13 program.<sup>78</sup>

**2.2. Methodological Decisions.** Comparison of the results obtained using different functionals *inter se* and with the experimental data led us to the decision to analyze the problem focusing on the LC- $\omega$ B97XD/aug-cc-pVTZ calculations. Thus, unless stated otherwise, we comment on only data obtained at this level. Data obtained with the other methods and all XYZ coordinates are collected in the Supporting Information (Tables S2 and S3, with XYZ coordinates, and Figures S1–S3).

Here, let us make a reservation that the aim of the study was to find semiquantitative relationships concerning molecules in the first excited singlet state rather than to determine exact values of their properties in the excited states. The discrepancies between theoretical predictions and the experimental data may be a result of inadequate theory or functionals, an insufficiency of the basis set, in general, or the description of some elements in particular, the absence of a medium, omission of a significant conformer, and several simplifications that are necessary to efficiently perform calculations for a few dozen molecules at a few theoretical levels. Note also that the direct comparison with experiment is rather hard, as the experimental data on the first excited singlet state of the monosubstituted benzenes are rarely available, except for the electronic spectra, which are not of interest here.

### 3. RESULTS AND DISCUSSION

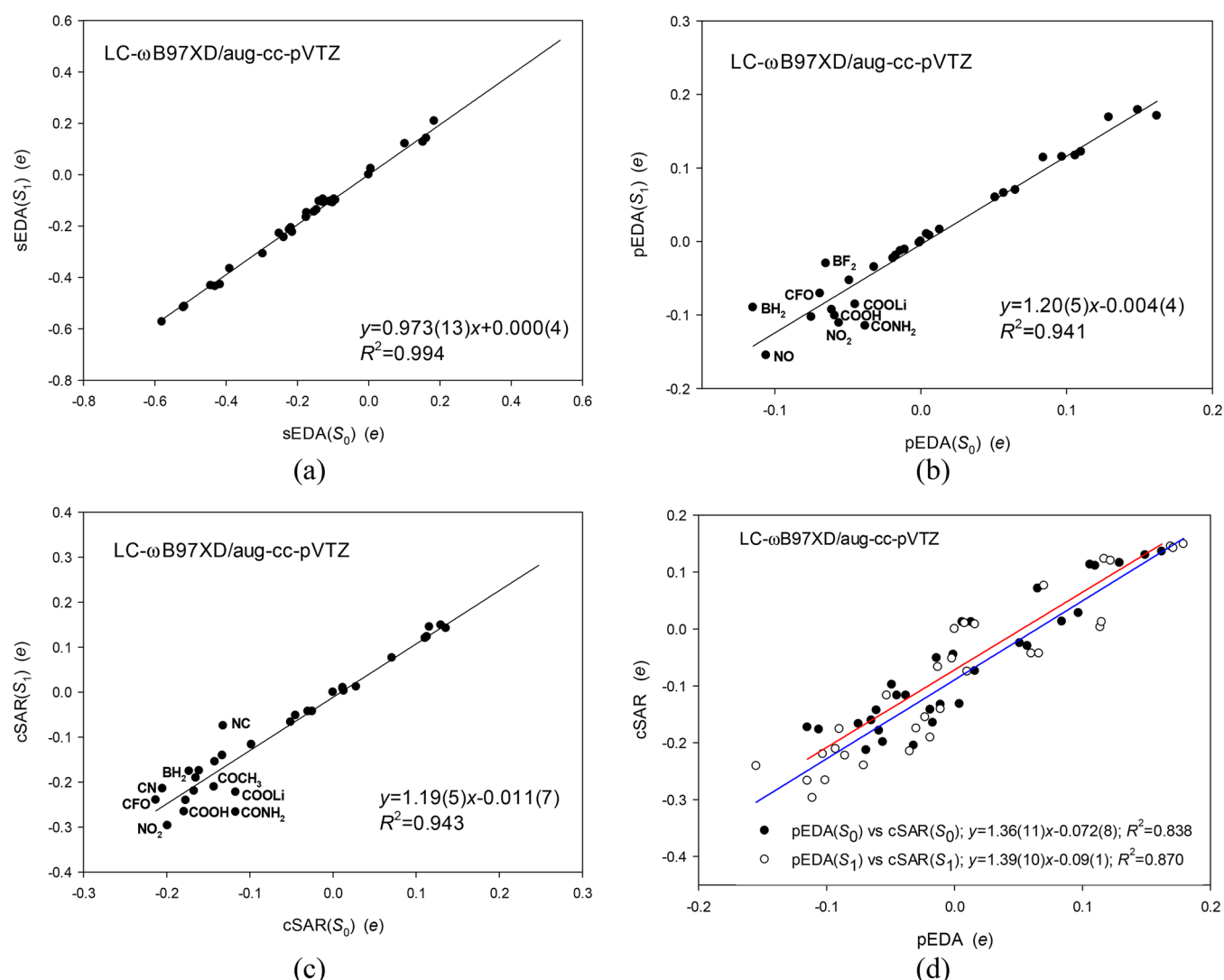
**3.1. Geometry.** Equilibrium geometries of molecules in the electronic excited states can be distinguishably different from those in their ground states.<sup>21</sup> In the case of the studied series of monosubstituted benzenes, the calculations predict three types of structural changes in the  $S_1$  state: (a) shortening of the C–X bond between the  $C_{\text{ipso}}$  atom and the first atom (X) of the substituent, (b) an increase in the lengths of the ring C–C bonds, and (c) planarization and deplanarization of the molecule. The first two tendencies conform qualitatively to the early experimental findings elucidated from microwave spectroscopy in the first excited singlet states.<sup>79</sup>

With respect to the C–X bond lengths,  $d(C\text{--}X)$  (Figure 1a), for most structures in the first excited singlet state, they are only

slightly shorter than in the ground state. However, for a few compounds, the  $d(C\text{--}X)$  values visibly differ between states. In the case of Li, this is the result of dissociation of the substituent from the ring in the  $S_1$  state. The prediction of such a dissociation is not unjustified, because even though phenyllithium is well-known<sup>80</sup> and used as a valuable reagent,<sup>81</sup> we have not found the fluorescence or even the UV spectra of this compound described so far in the literature. This may suggest that  $C_6H_5Li$  in the excited state is even less stable than in the ground state.

The C–X distances in the excited state deviate also from the correlation for three other types of compounds: (a)  $O=C\text{--}Y$  (where Y stands for H,  $CH_3$ , OH, OLi, or  $NH_2$ ), (b) Ph, and (c) NO and  $NO_2$  (Figure 1a). In all these cases, the C–X bond in the excited state is discernibly shorter than in the ground state and indicates an increase in double-bond character between C and X. When  $Y = OH$ , i.e., benzoic acid, the increase in the double-bond character of the  $C_{\text{ipso}}\text{--}C$  bond implies a smaller polarization of the OH bond and, as a consequence, a lower acidity in the  $S_1$  state than in the  $S_0$  state. This is in line with experimental results,<sup>49</sup> because the  $pK_a^*$  of benzoic acid is larger in the excited state than in the ground state and  $pK_a$  is inversely related to the acidity of a compound. The  $C_{\text{ipso}}\text{--}C$  shortening in the  $O=C\text{--}Y$  substituted benzenes is also predicted by the other DFT functionals applied and seems to agree, at least qualitatively, with the experimental trend.

For biphenyl, the shortening of the  $C_{\text{ipso}}\text{--}C'_{\text{ipso}}$  bond in the first excited state also agrees with predictions from several modern computational approaches, such as symmetry-adapted cluster configuration interaction (SAC-CI), complete active space self-consistent field (CASSCF), complete active space perturbation theory of the second order (CASPT2), and the time-dependent density functional theory (TD-DFT).<sup>82</sup> The  $1^1B_1$  state came out energetically lower than, nearly equal to, or higher than the almost degenerated  $1^1B_2$  and  $1^1B_3$  states depending on the theoretical level used, SAC-CI or TD-PBE0 (or for both SAC-CI and TD-PBE0). However, the  $C_{\text{ipso}}\text{--}C'_{\text{ipso}}$  distance in all those states was shorter than in the ground state.<sup>82</sup> Moreover, as in our calculations, the  $1^1B_1$  and  $1^1B_3$  states were planar, and the molecule in the  $1^1B_2$  state was less



**Figure 2.** Correlation between descriptors in the ground and first singlet states of monosubstituted benzenes: (a) sEDA, (b) pEDA, (c) and cSAR. (d) Correlation between the pEDA and cSAR descriptors in the ground and excited states. No points were excluded from correlations.

skewed. The predicted shortening of the C–N distance in the first excited singlet state of nitrobenzene also agrees with calculations performed at a level of theory higher than those used here: (EOM-) CCSD/cc-pVDZ<sup>83</sup> and CASPT2//CASSCF.<sup>84</sup> For nitrosobenzenes, we found no convincing computational evidence of its first excited-state geometry, but the CASPT2 calculations of the nitrosomethane structure in the first excited state suggest that the C–N distance is a bit shorter whereas the N–O distance is a bit longer than in the ground state.<sup>85</sup>

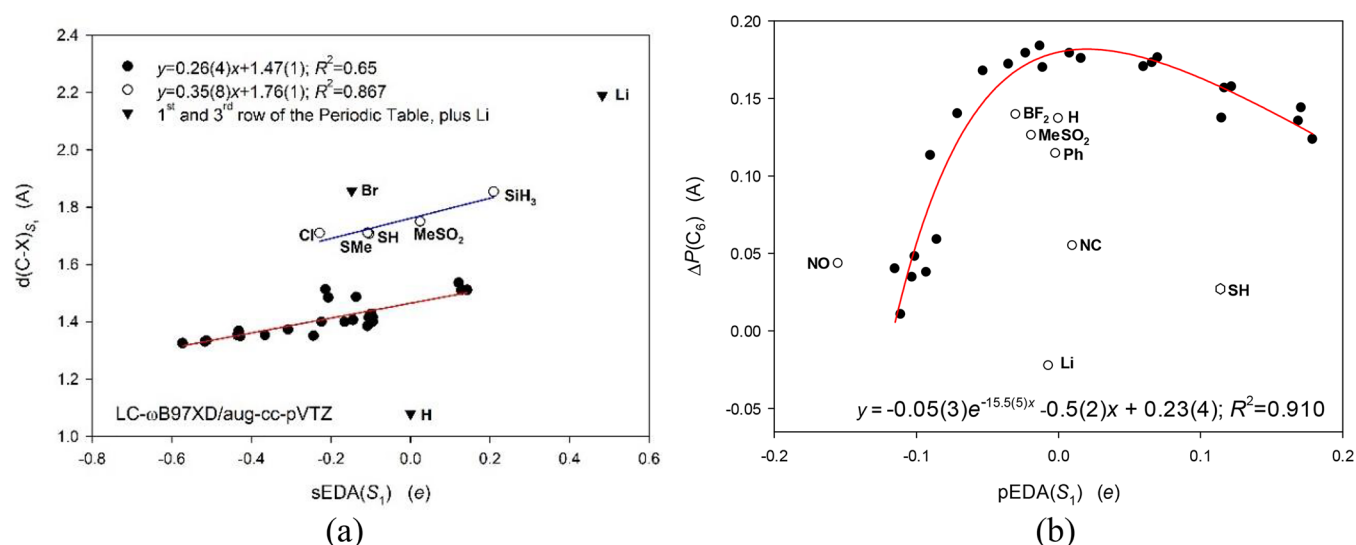
With regard to the ring C–C bonds, the excitation to the  $S_1$  state leads to a quite notable increase in their lengths. This can be seen in the increase in ring perimeter  $P(C_6)$ : the  $\Delta P(C_6) = P(C_6)(S_1) - P(C_6)(S_0)$  values are positive (Figure 1b). The increase is usually around 0.15(4) Å; however, for the NC- and SH-substituted benzenes and all previously mentioned deviating substituents, apart from Ph, it is <0.06 Å. For dissociated phenyllithium, the perimeter is predicted to be even smaller than in the ground state (Figure 1b). The presence of thiobenzene between molecules whose perimeter differences deviate from the general tendency is caused by a dissociation of the H atom from the SH group, in which the S–H distance

exceeds 1.95 Å. However, aromatic thiols tend to dissociate after photoexcitation at room temperature and form phenylthiyl radicals.<sup>86,87</sup> The presence of the NC-substituted molecule in this very group is not clear.

In the case of several substituents, the  $S_1$ -state minimum is predicted to have a nonplanar core ring, with the  $C_{\text{ipso}}$  and X atoms distorted from the ring plane [ $\tau(C_{\text{meta}}-C_{\text{ortho}}-C_{\text{ipso}}-X) \neq 0$ ]. This is seen for  $\text{BF}_2$  ( $\tau = -14.0^\circ$ ),  $\text{BH}_2$  ( $\tau = -13.8^\circ$ ),  $\text{CFO}$  ( $\tau = 9.7^\circ$ ),  $\text{MeSO}_2$  ( $\tau = 3.5^\circ$ ),  $\text{NMe}_2$  ( $\tau = 2.7^\circ$ ), and  $\text{SiH}_3$  ( $\tau = 2.6^\circ$ ). For  $\text{NMe}_2$ , distortion from the plane occurs despite an increase in the double-bond character of the  $C_{\text{ipso}}-\text{N}$  bond, which forces planarization of the substituent, yet simultaneously a hindrance between the substituent Me groups and H atoms in ortho positions is twisting the flat substituent by  $20^\circ$  from the plane. The absence of the Me groups or the presence of only one such group in  $\text{NH}_2$  and  $\text{NHMe}$  causes that the derivative remains flat. This seems to be in agreement with previous findings.<sup>88,89</sup> The other derivatives with the distorted ring plane were not analyzed experimentally, and this finding cannot be directly supported by measurements.

**3.2. Substituent Effect Descriptors for the First Excited Singlet State.** The  $\text{sEDA}(S_1)$ ,  $\text{pEDA}(S_1)$ , and





**Figure 3.** Correlation between (a) the C–X distance in monosubstituted benzenes in the  $S_1$  excited state and  $sEDA(S_1)$  and (b) the difference in ring perimeter  $\Delta P(C_6) = P(C_6)(S_1) - P(C_6)(S_0)$  with  $pEDA(S_1)$ . The empty circles in panel b denote points that were excluded from the presented correlations.

$cSAR(S_1)$  descriptors for the monosubstituted benzenes in the first excited singlet state were defined as for the ground state.<sup>57,58,62</sup> Recall that  $sEDA$  and  $pEDA$  descriptors are differences in C atom populations of  $\sigma$ - and  $\pi$ -valence orbitals in the substituted and unsubstituted benzene rings,<sup>62</sup> while  $cSAR$  is the sum of charges of the  $C_{ipso}$  and substituent atoms.<sup>57,58</sup> The former two descriptors express the amount of electrons donated to or withdrawn from the  $\sigma$ - and  $\pi$ -valence orbitals of the benzene ring by a substituent. They are linearly independent, which means that they reflect different properties of the ring.  $sEDA$  is a kind of group electronegativity and correlates with the electronegativity of the atom connecting the substituent with the ring and induction descriptors, whereas  $pEDA$  is a kind of resonance parameter that reveals the influence of the substituent on the  $\pi$ -electron system and correlates, for some systems, with aromaticity properties.<sup>63–65,90</sup> The  $cSAR$  descriptor is an overall characterization of the substituent itself and, simultaneously, of the substituted system. It correlates with some classical substituent effect descriptors and not strongly with  $pEDA$ .<sup>20,91–93</sup>

As the geometry changes in the  $S_1$  excited state, so does the charge distribution, and this is reflected in the distinct values of the substituent effect descriptors for the  $S_0$  and  $S_1$  states. Despite these differences, the ordering of the substituents according to the parameters is retained, and the values for the  $S_0$  and  $S_1$  states are highly correlated (Figure 2a–c).

This is especially true for the  $sEDA$  descriptor, where the correlation is close to perfect ( $R^2 = 0.994$ ) and no outliers are present (Figure 2a). Nevertheless, on average, the  $sEDA(S_1)$  is 0.973 times the ground-state descriptor, so we can conclude that in the first excited state, the effect on the ring  $\sigma$ -valence system of both  $\sigma$ -electron-donating and  $\sigma$ -electron-withdrawing groups is a bit weaker than in the ground state.

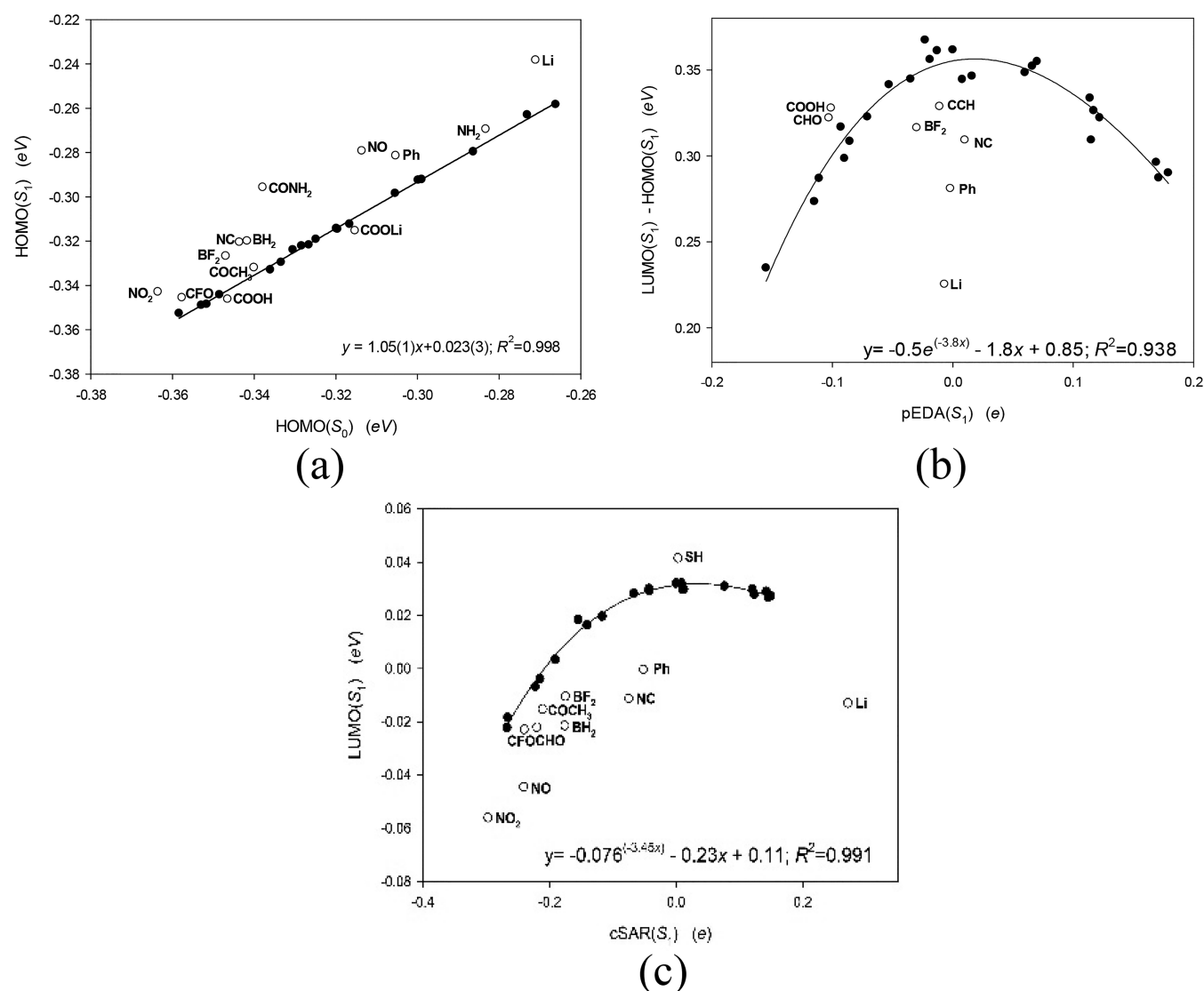
In the case of  $pEDA$  and  $cSAR$ , a noticeable group of outliers is seen when the  $S_1$  and  $S_0$  values are regressed (Figure 2b,c). In a majority, the deviating derivatives are these that were previously recognized as having significantly shorter C–X bond lengths (i.e., an increased double-bond character) or  $C_{ipso}$  and X atoms distorted from the ring plane. If some outliers would be excluded, the remaining points could give almost

perfect correlations between  $S_1$  and  $S_0$  values, with  $R^2$  increased from 0.941 to 0.991 and from 0.943 to 0.997 for  $pEDA$  and  $cSAR$ , respectively.

$pEDA(S_1)$  changes on average by a factor of 1.13 compared to  $pEDA(S_0)$ . Thus, in the first excited state, the resonance effect of both  $\pi$ -electron-donating and  $\pi$ -electron-withdrawing groups is a bit stronger than in the ground state. A similar trend is observed for the  $cSAR$  descriptors, which change in the  $S_1$  state by a factor of  $\sim 1.11$ . The conclusions for  $pEDA$  and  $cSAR$  do not apply to the group of outlying substituents, for a majority of which the change is even greater. This group should be considered with greater caution.

Finally, we observed that the similar magnitude of slopes in linear correlations for  $pEDA$  and  $cSAR$  descriptors (Figure 2b,c) is not accidental. Indeed, these descriptors are positively linearly correlated in both ground and excited states (Figure 2d). The positive value of  $pEDA$  denotes the electron-donating character of the substituent, while the positive  $cSAR$  denotes the positive charge of the substituent's active region. Hence, the physical interpretation of the correlations presented in Figure 2d is as follows: the more charge is given to the benzene  $\pi$ -electron system by a substituent (an increase in  $pEDA$ ), the more positive the substituent becomes (an increase in  $cSAR$ ). The dispersion of points around this correlation is a result of the consideration of only the  $\pi$ -valence electrons in  $pEDA$  and the significant contribution of  $\sigma$ -valence orbitals of the  $C_{ipso}$  and substituent atom charges in  $cSAR$ .

**3.3. Description of the Geometry by Using the Substituent Effect Parameters.** The substituent effect descriptors  $sEDA$  and  $pEDA$  can be used to describe some of the molecular properties of the considered monosubstituted benzenes, both in the ground state and in the  $S_1$  excited state. First, let us indicate a “natural” measure of the substituent effect on the benzene  $\sigma$ -electron system in the ground state. The  $d(C-X)$  distance in the ground state correlates with the  $sEDA(S_0)$  descriptor, yet the correlation is split according to the period to which the connecting X atom belongs (Figure S4). Among the substituents considered here, only X = H belongs to the first period, the substituents for which X = F, N, C, B, and Li belong to the second period, those for which X =



**Figure 4.** Correlations between (a) HOMO energies of the  $S_0$  and  $S_1$  states, (b) the HOMO–LUMO energy difference in the  $S_1$  excited state and  $pEDA(S_1)$ , and (c) the LUMO energy in the  $S_1$  excited state and  $cSAR(S_1)$ . The empty circles are the exceptional points that were excluded from the presented correlations (see the text).

Cl, S, Si, and Na belong to the third, and only X = Br belongs to the fourth. Notice that the slopes of the linear correlations for the substituents from the second and third periods are the same,  $0.29 \pm 0.03$ , while intercepts differ by 0.29, as they are  $1.520 \pm 0.008$  and  $1.809 \pm 0.005$ , respectively (Figure S4).

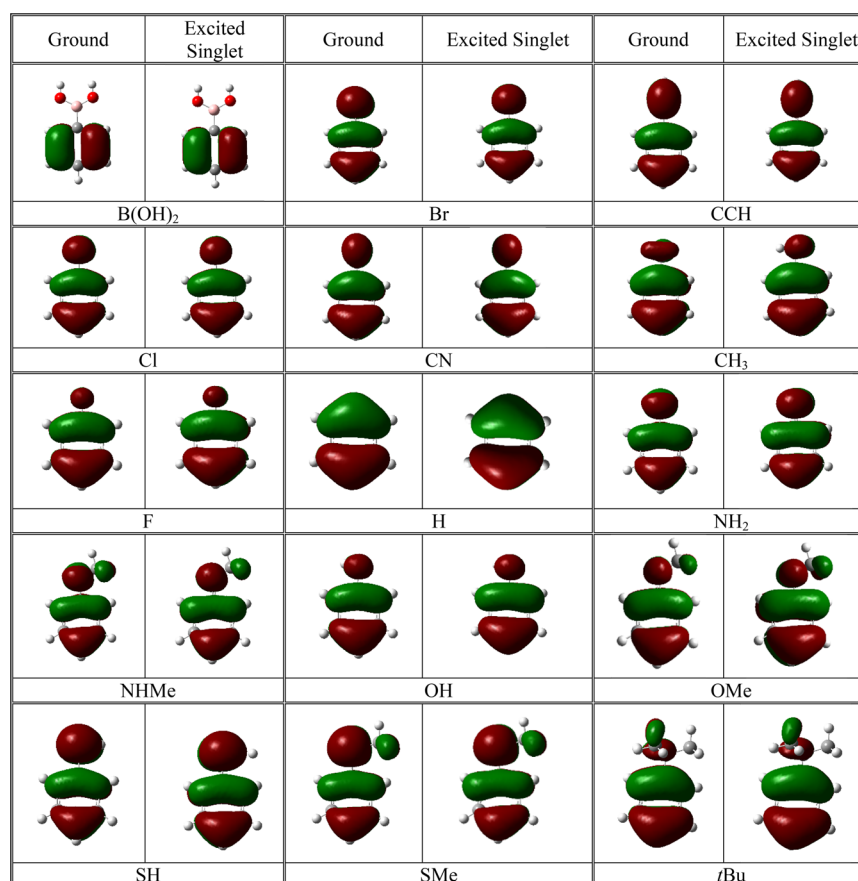
A quite similar picture can be drawn for the first singlet state (Figure 3a). However, the dispersion of points around the straight lines is a bit larger, yet the slope value for the ground state, 0.29, is within the confidence interval of the first excited-state slopes,  $0.35 \pm 0.08$  and  $0.26 \pm 0.04$ , and the corresponding intercepts for the substituents with atoms of the second and third periods,  $1.47 \pm 0.01$  and  $1.76 \pm 0.01$ , are very close to those from the ground state, as well.

We again considered the changes of the ring perimeter after excitation,  $\Delta P(C_6)$ , which in the plot against the C–X distance reveal only a clustering of points around 0.15 and  $<0.06$  Å (Figure 1b). The change  $\Delta P(C_6)$  seems to be correlated with ground-state  $pEDA(S_0)$  only after the exclusion of several substituents (Figure S4), while with  $pEDA(S_1)$ , it can be modeled with an asymmetric nonlinear function (Figure 3b). The asymmetry consists of a quickly increasing wing for the  $\pi$ -

electron-withdrawing substituents ( $pEDA < 0$ ), a flattened maximum around  $pEDA = 0$ , and a slowly decreasing wing for the  $\pi$ -electron-donating substituents ( $pEDA > 0$ ) (Figure 3b).

We have recently interpreted similar asymmetric changes in a study devoted to the non-additivity of the substituent effect in disubstituted benzenes and pyridines.<sup>94,95</sup> These aromatic molecules are rich in  $\pi$ -electrons. For these molecules, a donation or withdrawal of electrons can be compared to an “attempt to push a passenger into or pull out from a crowded Tokyo train. The former process requires a great effort, while the latter needs much less energy if it is not a barrierless operation”.<sup>95</sup> Thus, withdrawing  $\pi$ -electrons from the benzene ring is an easy process, as seen in the steep left wing of the function, while donation of  $\pi$ -electrons to the electron-rich system is a difficult process, represented by the slowly descending right wing of the function (Figure 3b).

In the case of using the classical substituent constants for correlating the described geometrical elements of the  $S_1$  excited state, it seems that no obvious relationships are present (Figures S5 and S6).

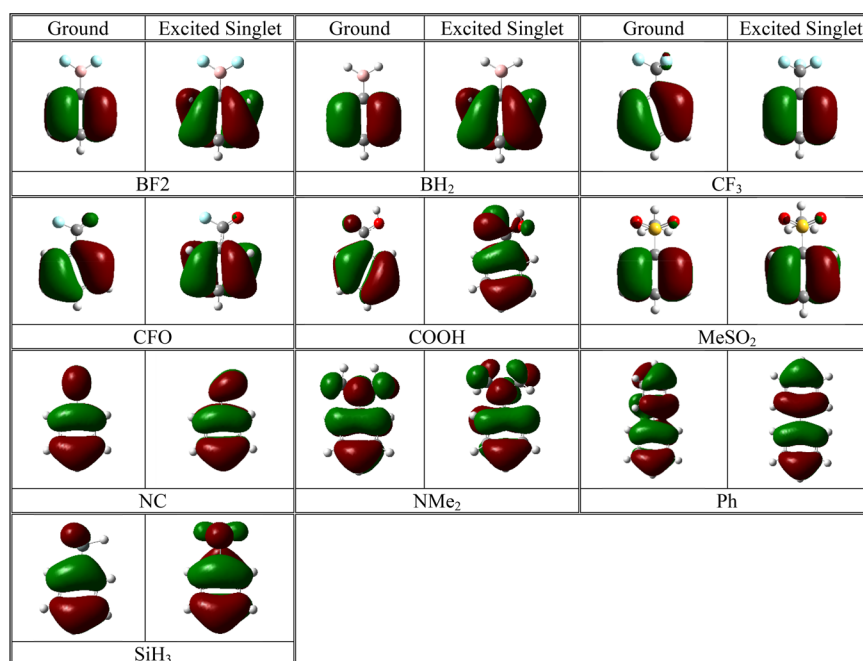


**Figure 5.** Comparison of the shapes of HOMO orbitals in the ground  $S_0$  and first excited  $S_1$  states of the monosubstituted benzenes assigned to the first group of substituents.

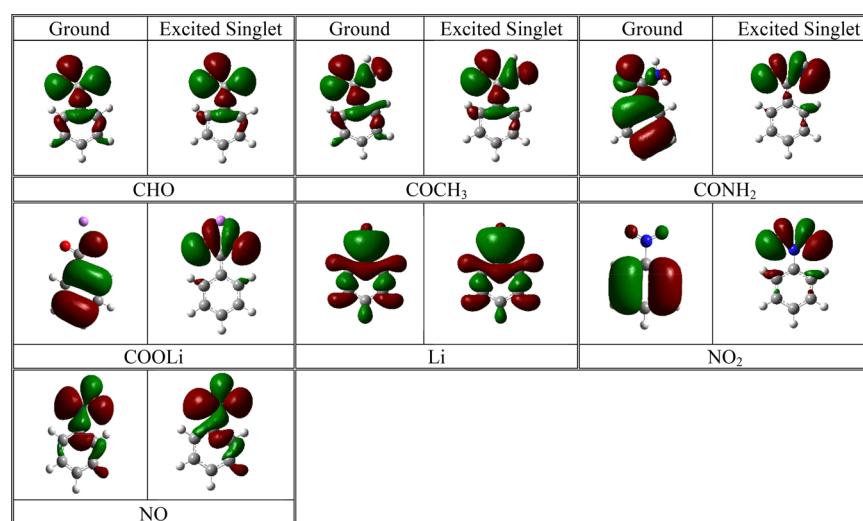
**3.4. Substituent Effect Descriptors and Frontier Molecular Orbitals.** Analyses of the highest occupied and lowest unoccupied molecular orbitals and the gap between them (HOMO, LUMO, and the HOMO–LUMO gap, respectively) have played a very important role in chemistry,<sup>96–100</sup> even though the energy of HOMO is only a rough approximation of the ionization potential defined by Koopmans based on the simple Hartree–Fock theory.<sup>101,102</sup> At the same time, the unoccupied LUMO orbitals do not even have a well-founded physical basis and cannot be interpreted as a first estimation of the electron affinities. Nevertheless, it has recently been shown that, at a sufficiently accurate DFT level, the HOMO–LUMO gap is close to the first excitation energy, i.e., the optical gap.<sup>103,104</sup> Moreover, within the framework of time-dependent DFT, it is also possible to formulate a generalized Koopmans theorem valid for the excited states.<sup>105,106</sup> Therefore, let us show some of the relations between HOMO and LUMO energies of the  $S_0$  and  $S_1$  states and the substituent effect descriptors (Figure 4 and Figure S7), keeping in mind the objections that may be raised against their use from a purely theoretical point of view. Although referring to frontier orbitals of the excited state is still rare,<sup>107</sup> we believe that as new computational methods for the characterization of excited states are developed, referring to these orbitals will be increasingly common, for example, to estimate the softness and hardness of molecules<sup>108</sup> or their conductivity properties.<sup>100</sup>

First, it seems that descriptors defined for the ground state and those defined for the  $S_1$  state are equally adequate for

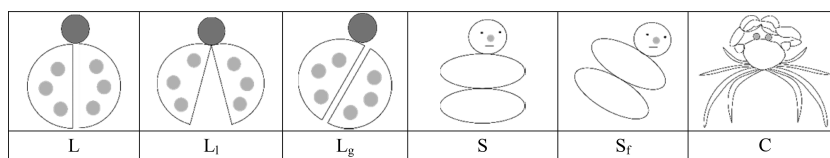
analyzing the effect of the substituent on the energy of and gap between frontier orbitals in the latter state. Indeed, already considering all the HOMO, LUMO, and HOMO–LUMO gap values, without the exclusion of any properly optimized structure in both  $S_0$  and  $S_1$  states, one can obtain some fair correlations ( $R^2 \approx 0.7 \pm 0.1$ ) between these values and pEDA and cSAR descriptors defined for the appropriate states (Tables S2 and S3). Second, if some points are excluded from analysis, it appears that there are linear correlations between energies of the frontier orbitals in the  $S_0$  and  $S_1$  states and the gap between them (Figure 4a and Figure S7). This means that, except for some substituents, one can easily predict the HOMO, LUMO, and HOMO–LUMO gap energies of the excited  $S_1$  state if one already knows the analogous values for the ground state. Again, the outlying points correspond to the same molecules that produced outliers in previously discussed correlations. Third, a careful look at the correlations of HOMO( $S_1$ ), LUMO( $S_1$ ), and HOMO( $S_1$ )–LUMO( $S_1$ ) gap energies with pEDA( $S_1$ ) and cSAR( $S_1$ ) descriptors (Figure 4b,c and Figure S7) reveals quite consistent and statistically significant trends accompanying the same groups of deviating points. Correlations with the pEDA( $S_1$ ) descriptor exhibit an  $R^2$  coefficient of  $>0.85$  (Figure S7), while for the gap, it is even more significant and equals 0.938 (Figure 4b). The correlation of HOMO( $S_1$ ) with cSAR( $S_1$ ) is weaker [ $R^2 = 0.7$  (Figure S7)]. cSAR( $S_1$ ) is also likely uncorrelated with the gap (Figure S7). However, its correlation with LUMO( $S_1$ ) energies is impressive [ $R^2 = 0.99$  (Figure 4c)]. Again, the classical substituent constants do not seem to correlate (at least in a straightforward manner) with



**Figure 6.** Comparison of the shapes of HOMO orbitals in the ground  $S_0$  and first excited  $S_1$  states of the monosubstituted benzenes assigned to the second group of substituents.



**Figure 7.** Comparison of the shapes of HOMO orbitals in the ground  $S_0$  and first excited  $S_1$  states of the monosubstituted benzenes assigned to the third group of substituents.



**Figure 8.** Nicknames of the shapes of HOMO orbitals in the ground  $S_0$  and first excited  $S_1$  states of the studied monosubstituted benzenes.

the calculated energies of the frontier orbitals (Figures S8 and S9).

The findings presented above prompted us to look for an explanation for why some of the substituted benzenes deviate from the regular patterns of changes in the shape of their frontier orbitals between the ground and first excited states (Figures 5–7 and Figure S10).

Inspection of Figures 5–7 reveals three general groups of substituents that can be classified according to the qualitative degree to which a HOMO orbital is changed after undergoing a transition to the first excited state: (I) nearly unchanged, (II) slightly changed, and (III) drastically changed or drastically deviating from the  $\pi$ -form. It is clear that the borders between the groups are fuzzy. The following substituents belong to



group I: B(OH)<sub>2</sub>, Br, CCH, CH<sub>3</sub>, Cl, CN, F, H, NH<sub>2</sub>, NHMe, OH, OMe, SH, SMe, and *t*Bu. The following substituents belong to group II: BF<sub>2</sub>, BH<sub>2</sub>, CF<sub>3</sub>, CFO, COOH, MeSO<sub>2</sub>, NC, NMe<sub>2</sub>, Ph, and SiH<sub>3</sub>. The following substituents belong to group III: CHO, COCH<sub>3</sub>, CONH<sub>2</sub>, COOLi, Li, NO<sub>2</sub>, and NO. The substituents from the first group, apart from SH, do not show up as deviating points in the plots discussed above and require no comment other than a reminder that, at the applied level of theory, in the excited state the H atom is predicted to dissociate from the SH group, which finds some experimental grounds.<sup>86,87</sup> The shapes of the HOMO orbitals of derivatives assigned to the next two groups need more attention.

To facilitate the discussion of HOMO orbital shapes, it is useful to introduce a set of symbolic depictions and nicknames. Thus, the observed HOMO shapes can be classified into L, S, and C shapes, after a ladybird, a snowman, and a crab, respectively (Figure 8). The L shape has two more versions, L<sub>1</sub> and L<sub>g</sub>, as in a ladybird launching into flight and one that is glancing around. The S shape also has the S<sub>f</sub> version of a falling snowman. Note that the first group of substituents exhibits only the unindexed L or S shapes (Figure 5). For benzene derivatives from the first group, the transition from the S<sub>0</sub> to S<sub>1</sub> state occurs without a change in the HOMO shape type, which can schematically be written as L(S<sub>0</sub>) → L(S<sub>1</sub>) or S(S<sub>0</sub>) → S(S<sub>1</sub>). The substituents from the first group do not deviate from the correlations shown in Figures 1–4.

In group II (Figure 6), the HOMO orbitals of BF<sub>2</sub>, BH<sub>2</sub>, and MeSO<sub>2</sub> derivatives transform according to an L(S<sub>0</sub>) → L<sub>1</sub>(S<sub>1</sub>) scheme; however, the change for MeSO<sub>2</sub> is rather weak. The CF<sub>3</sub>- and CFO-substituted derivatives change according to the L<sub>g</sub>(S<sub>0</sub>) → L(S<sub>1</sub>) and L<sub>g</sub>(S<sub>0</sub>) → L<sub>1</sub>(S<sub>1</sub>) schemes, respectively. The HOMOs of the NC and SiH<sub>3</sub> derivatives transform according to the S(S<sub>0</sub>) → S<sub>f</sub>(S<sub>1</sub>) and S<sub>f</sub>(S<sub>0</sub>) → S(S<sub>1</sub>) schemes, respectively. The diphenyl (X = Ph) is skewed in the ground state but flat in the first singlet state, and the transformation of its HOMO orbitals can be classified as an S<sub>f</sub>(S<sub>0</sub>) → S(S<sub>1</sub>) transition; on the other hand, NMe<sub>2</sub> is twisted by 20° in the S<sub>1</sub> state, as a result of the repulsion between Me groups and ortho H atoms, and the transformation of its HOMO shape can also be classified as an S(S<sub>0</sub>) → S<sub>f</sub>(S<sub>1</sub>) transition. In this group, only the HOMO of COOH changes according to an L<sub>g</sub>(S<sub>0</sub>) → S(S<sub>1</sub>) transition, but one can say that, in the limit, the L<sub>g</sub> orbital type approaches the S one.

The changes in the HOMO orbital shapes observed in group III are the largest (Figure 7). Only in this group do some HOMO orbitals adopt the C type located on the substituent more than on the ring. For all substituents of this group, at least one HOMO is of the C shape. Indeed, the HOMO orbitals of the CHO-, COCH<sub>3</sub>-, and NO-substituted benzenes transform as C(S<sub>0</sub>) → C(S<sub>1</sub>); the CONH<sub>2</sub>, COOLi, and NO<sub>2</sub> ones transform as S<sub>f</sub>(S<sub>0</sub>) → C(S<sub>1</sub>) and L(S<sub>0</sub>) → C(S<sub>1</sub>).

Thus, with the change in the electronic state from the ground to the first excited singlet state, the HOMO orbitals in group I of the substituents conserve both the type and index of the shape. Transformations of the orbitals of group II, apart from COOH, conserve the orbital type but change the shape index, whereas at least one of the HOMO orbitals in group III belongs to the C type.

Now, consider the symmetry of the HOMO orbitals and the degree of their perturbations in the transformation from the S<sub>0</sub> to S<sub>1</sub> state. Notice that in group I, the HOMO orbitals in the two states are almost perfectly antisymmetric with respect to the benzene plane (Figure 5). Even if the antisymmetry seems

to be slightly imperfect for *t*Bu, one should remember that *t*Bu rotations average out the irregularities. In the case of the L<sub>1</sub> type of orbitals present in group II of the substituents, the antisymmetry with respect to the benzene plane is notably perturbed [see BF<sub>2</sub>, BH<sub>2</sub>, CFO, and MeSO<sub>2</sub> in S<sub>1</sub> states (Figure 6)]. The antisymmetry is also visibly imperfect for skewed structures, such as Ph in the ground state and NMe<sub>2</sub> in the excited state (Figure 6). Also, antisymmetrization following substituent rotation does not occur because, in the S<sub>1</sub> state, functional groups such as SiH<sub>3</sub>, CF<sub>3</sub>, MeSO<sub>2</sub>, BF<sub>2</sub>, and BH<sub>2</sub> significantly diverge from the benzene plane (which cannot be seen in small pictures, such as Figure 6). In the cases of COOH and NC, the HOMO antisymmetry in each state is conserved, but after excitation, the C–C(OOH) bond is significantly shortened and the C–NC group becomes significantly bent. Therefore, the excitation causes notable changes in the HOMO charge distribution and deviations in Figures 5–7. For group III of the substituents with C-shaped HOMO orbitals, the situation is different: they are symmetric with respect to the ring plane, and for this reason they cannot be identified as  $\pi$ -orbitals, which are antisymmetric; thus, the properties of molecules should not follow the changes described by pEDA.

Let us now consider the question of whether ground-state descriptors can successfully describe the properties of molecules in the first excited singlet state. The answer is differentiated with regard to the substituent group. There is a large set of substituents, group I, i.e., B(OH)<sub>2</sub>, Br, CCH, CH<sub>3</sub>, Cl, CN, F, H, NH<sub>2</sub>, NHMe, OH, OMe, SH, SMe, and *t*Bu, for which the transition from the ground to the excited state conserves the shape of the HOMO orbital with an almost perfect antisymmetry with respect to the benzene plane (characteristic for  $\pi$ -orbitals). For them, the substituent effect appears to be correlated with both the first singlet excited-state descriptors and ground-state ones, which, in turn, are intercorrelated.

However, there are two groups of substituents that produce notable deviations from substituent effect correlations. One of them, group II (BF<sub>2</sub>, BH<sub>2</sub>, CF<sub>3</sub>, CFO, COOH, MeSO<sub>2</sub>, NC, NMe<sub>2</sub>, Ph, and SiH<sub>3</sub>), contains substituents that have a  $\pi$ -character of the HOMO orbitals in both states, but a transition between the states either significantly perturbs the antisymmetry of HOMO in one of the states or significantly changes the shape of part of the orbital. The perturbation can be connected with skewing the molecule in one of the states (NMe<sub>2</sub> and Ph), distorting the substituent from the benzene plane in the excited state (BF<sub>2</sub>, BH<sub>2</sub>, CF<sub>3</sub>, CFO, MeSO<sub>2</sub>, and SiH<sub>3</sub>), significantly shortening the connecting bond (COOH), or bending the substituent in the excited state, as in NC. The substituents from this group sometimes deviate from the correlations only slightly, as for CFO, CF<sub>3</sub>, COOH or MeSO<sub>2</sub>, and NMe<sub>2</sub>, and other times they may deviate a lot, as in the case of Ph or NC. This group of substituents in the excited states seems to require more attention and a careful approach when modeled with the substituent effect descriptors derived be it at the S<sub>0</sub> state or the S<sub>1</sub> state. The substituents from group III (CHO, COCH<sub>3</sub>, CONH<sub>2</sub>, Li, NO<sub>2</sub>, and NO) may be expected to always deviate from the correlations. For them, one or both HOMO states have a  $\sigma$ -character, and therefore, the derivatives substituted with these substituents do not follow trends designated by resonance effect descriptors such as pEDA. As a result, regardless of whether ground- or excited-state resonance descriptors are used, it would not be proper to proclaim

common tendencies for derivatives of electronic structures drastically different from those of the previous two groups.

#### 4. CONCLUSIONS

The sEDA, pEDA, and cSAR descriptors of the substituent effect were determined for >30 monosubstituted benzenes in the first excited singlet  $S_1$  state calculated at the LC- $\omega$ B97XD/aug-cc-pVTZ level. sEDA is a kind of group electronegativity; pEDA is a kind of resonance parameter, and cSAR is an overall characterization of the substituent itself.

A juxtaposition of the  $C_{\text{ipso}}-X$  distance and the difference in ring perimeters in the ground and  $S_1$  states shows that the  $d(C-X)$  changes are not large, while most of the ring perimeters notably increase. A comparison of the  $S_0$ - and  $S_1$ -state descriptors indicates that, in the  $S_1$  state, the  $\sigma$ -valence electrons (sEDA) are somewhat less affected whereas the  $\pi$ -electron system (pEDA) and the charge localized at the substituent (cSAR) are somewhat more affected than in the ground state. However, the shift of  $\sigma$ -electrons,  $\pi$ -electrons, and substituent electrons in both states remains qualitatively identical. The regression of the  $d(C-X)$  distance in the  $S_0$  and  $S_1$  states against the sEDA( $S_0$ ) and sEDA( $S_1$ ) descriptors, respectively, demonstrates that, for these two states, there are distinct linear correlations depending on the period to which the X atom belongs and the C–X distance can be used as a kind of “natural” substituent effect descriptor of group electro-negativity in a given electronic state. On the other hand, changes in the ring perimeter after excitation follow a weak, quadratic correlation when plotted against the pEDA( $S_0$ ) descriptor, and a much stronger, but asymmetric and nonlinear, correlation when plotted against the pEDA( $S_1$ ) descriptor. The reason for this asymmetry lies in differences between withdrawing and donating electrons to an electron-rich system.

The energies of the HOMO and LUMO orbitals and the HOMO–LUMO gap in the  $S_0$  and  $S_1$  states linearly correlate; however, there are several deviating points, the same ones that were also outliers in the previous correlations. The energies of the HOMO( $S_1$ ), LUMO( $S_1$ ), and HOMO( $S_1$ )–LUMO( $S_1$ ) gap also seem to correlate, more or less significantly, with the pEDA( $S_1$ ) and cSAR( $S_1$ ) descriptors, and again, the same group of substituents deviates from these correlations.

A comparison of the shape of the HOMO( $S_0$ ) and HOMO( $S_1$ ) orbitals led to the conclusion that the set of considered substituents contains three distinct subsets: (I) B(OH)<sub>2</sub>, Br, CCH, CH<sub>3</sub>, Cl, CN, F, H, NH<sub>2</sub>, NHMe, OH, OMe, SH, SMe, and *t*Bu, for which the transition from the ground to the excited state conserves the shape of the HOMO orbital with almost perfect antisymmetry with respect to the benzene plane; (II) BF<sub>2</sub>, BH<sub>2</sub>, CF<sub>3</sub>, CFO, COOH, MeSO<sub>2</sub>, NC, NMe<sub>2</sub>, Ph, and SiH<sub>3</sub>, for which the transition either significantly perturbs the antisymmetry of HOMO in one of the states or notably changes the shape of part of the orbital; and (III) CHO, COCH<sub>3</sub>, CONH<sub>2</sub>, Li, NO<sub>2</sub>, and NO, for which one or both HOMO states have the  $\sigma$ -character and, therefore, the derivatives substituted by these substituents do not follow trends designated by resonance effect descriptors such as pEDA.

Therefore, the answer to whether it is possible to use ground-state substituent descriptors to study the first excited singlet-state properties is a conditional one and depends on the substituent group under consideration. The ground-state descriptors should be adequate for group I. In the case of group II, more care is required when modeling the excited-state

properties. Group III can be expected to always deviate from correlations.

#### ■ ASSOCIATED CONTENT

##### Supporting Information

The Supporting Information is available free of charge on the ACS Publications website at DOI: 10.1021/acs.jpca.8b02209.

Literature review pertaining to the substituent effect on the excited-state properties, route section commands of the performed calculations, total energies of the studied molecules, tables containing the calculated substituent effect descriptor values, plots of correlations of minor importance, and a comparison of the shapes of LUMO orbitals and tables with XYZ coordinates of  $S_0$  and  $S_1$  structures (PDF)

#### ■ AUTHOR INFORMATION

##### Corresponding Author

\*National Medicines Institute, 30/34 Chełmska St., 00-725 Warsaw, Poland. E-mail: j.dobrowolski@nil.gov.pl

##### ORCID

Jan Cz. Dobrowolski: 0000-0002-7301-1590

##### Notes

The authors declare no competing financial interest.

#### ■ ACKNOWLEDGMENTS

This project was supported by the NMI statutory funds for 2017. The computational grant from the Swierk Computing Centre (CIŚ) is gratefully acknowledged. The authors thank Mr. Mateusz Nawara for his help with English language corrections.

#### ■ REFERENCES

- (1) Wong, M. Y.; Zysman-Colman, E. Purely Organic Thermally Activated Delayed Fluorescence Materials for Organic Light-Emitting Diodes. *Adv. Mater.* **2017**, *29*, 1605444.
- (2) Godumala, M.; Choi, S.; Cho, M. J.; Choi, D. H. Thermally Activated Delayed Fluorescence Blue Dopants and Hosts: From the Design Strategy to Organic Light-Emitting Diode Applications. *J. Mater. Chem. C* **2016**, *4*, 11355–11381.
- (3) Doddi, S.; Ramakrishna, B.; Venkatesh, Y.; Bangal, P. R. Photo-Driven near-IR Fluorescence Switch: Synthesis and Spectroscopic Investigation of Squaraine-Spiropyran Dyad. *RSC Adv.* **2015**, *5* (118), 97681–97689.
- (4) Liu, H.; Zhou, Y.; Yang, Y.; Wang, W.; Qu, L.; Chen, C.; Liu, D.; Zhang, D.; Zhu, D. Photo-pH Dually Modulated Fluorescence Switch Based on DNA Spatial Nanodevice. *J. Phys. Chem. B* **2008**, *112*, 6893–6896.
- (5) Chu, T. S.; Lü, R.; Liu, B. T. Reversibly Monitoring Oxidation and Reduction Events in Living Biological Systems: Recent Development of Redox-Responsive Reversible NIR Biosensors and Their Applications in Vitro/in Vivo Fluorescence Imaging. *Biosens. Bioelectron.* **2016**, *86*, 643–655.
- (6) Wegner, K. D.; Hildebrandt, N. Quantum Dots: Bright and Versatile *in vitro* and *in vivo* Fluorescence Imaging Biosensors. *Chem. Soc. Rev.* **2015**, *44*, 4792–4834.
- (7) Zhou, Y.; Zhang, J. F.; Yoon, J. Fluorescence and Colorimetric Chemosensors for Fluoride-Ion Detection. *Chem. Rev.* **2014**, *114*, 5511–5571.
- (8) Li, J.; Yim, D.; Jang, W.-D.; Yoon, J. Recent Progress in the Design and Applications of Fluorescence Probes Containing Crown Ethers. *Chem. Soc. Rev.* **2017**, *46*, 2437–2458.

- (9) Shashkova, S.; Leake, M. C. Single-Molecule Fluorescence Microscopy Review: Shedding New Light on Old Problems. *Biosci. Rep.* **2017**, *37*, BSR20170031.
- (10) Ji, N. Adaptive Optical Fluorescence Microscopy. *Nat. Methods* **2017**, *14*, 374–380.
- (11) Deschout, H.; Zancchi, F. C.; Młodzianowski, M.; Diaspro, A.; Bewersdorf, J.; Hess, S. T.; Braeckmans, K. Precisely and Accurately Localizing Single Emitters in Fluorescence Microscopy. *Nat. Methods* **2014**, *11*, 253–266.
- (12) Laissue, P. P.; Alghamdi, R. A.; Tomancak, P.; Reynaud, E. G.; Shroff, H. Assessing Phototoxicity in Live Fluorescence Imaging. *Nat. Methods* **2017**, *14*, 657–661.
- (13) Jenkins, R.; Burdette, M. K.; Foulger, S. H. Mini-Review: Fluorescence Imaging in Cancer Cells Using Dye-Doped Nanoparticles. *RSC Adv.* **2016**, *6*, 65459–65474.
- (14) DSouza, A. V.; Lin, H.; Henderson, E. R.; Samkoe, K. S.; Pogue, B. W. Review of Fluorescence Guided Surgery Systems: Identification of Key Performance Capabilities beyond Indocyanine Green Imaging. *J. Biomed. Opt.* **2016**, *21*, 080901.
- (15) Vahrmeijer, A. L.; Hutteman, M.; van der Vorst, J. R.; van de Velde, C. J. H.; Frangioni, J. V. Image-Guided Cancer Surgery Using near-Infrared Fluorescence. *Nat. Rev. Clin. Oncol.* **2013**, *10*, 507–518.
- (16) Lv, G.; Guo, W.; Zhang, W.; Zhang, T.; Li, S.; Chen, S.; Eltahan, A. S.; Wang, D.; Wang, Y.; Zhang, J.; Wang, P. C.; Chang, J.; Liang, X.-J. Near-Infrared Emission CuInS/ZnS Quantum Dots: All-in-One Theranostic Nanomedicines with Intrinsic Fluorescence/Photoacoustic Imaging for Tumor Phototherapy. *ACS Nano* **2016**, *10*, 9637–9645.
- (17) Fraix, A.; Kandath, N.; Manet, I.; Cardile, V.; Graziano, A. C. E.; Gref, R.; Sortino, S. An Engineered Nanoplatfor for Bimodal Anticancer Phototherapy with Dual-Color Fluorescence Detection of Sensitizers. *Chem. Commun.* **2013**, *49*, 4459–4461.
- (18) Romero, N. A.; Nicewicz, D. A. Organic Photoredox Catalysis. *Chem. Rev.* **2016**, *116*, 10075–10166.
- (19) Margrey, K. A.; Levens, A.; Nicewicz, D. A. Direct Aryl C–H Amination with Primary Amines Using Organic Photoredox Catalysis. *Angew. Chem., Int. Ed.* **2017**, *56*, 15644–15648.
- (20) Hansch, C.; Leo, A.; Taft, R. W. A Survey of Hammett Substituent Constants and Resonance and Field Parameters. *Chem. Rev.* **1991**, *91*, 165–195.
- (21) Hoffmann, R. Geometry Changes in Excited States. *Pure Appl. Chem.* **1970**, *24*, 567–584.
- (22) Jaffé, H. H.; Jones, H. L. Excited State pK Values. III. The Application of the Hammett Equation. *J. Org. Chem.* **1965**, *30*, 964–969.
- (23) Wehry, E. L.; Rogers, L. B. Application of Linear Free Energy Relations to Electronically Excited States of Monosubstituted Phenols. *J. Am. Chem. Soc.* **1965**, *87*, 4234–4238.
- (24) Hrdlovič, P.; Belluš, D.; Lazar, M. Dissociation Constants of 2-Hydroxybenzophenone Derivatives in Ground and Excited States. *Collect. Czech. Chem. Commun.* **1968**, *33*, 59–67.
- (25) Driscoll, E. W.; Hunt, J. R.; Dawlaty, J. M. Photobasicity in Quinolines: Origin and Tunability via the Substituents' Hammett Parameters. *J. Phys. Chem. Lett.* **2016**, *7*, 2093–2099.
- (26) Kosower, E. M.; Dodiuk, H.; Tanizawa, K.; Ottolenghi, M.; Orbach, N. Intramolecular Donor-Acceptor Systems. Radiative and Nonradiative Processes for the Excited States of 2-N-Arylamino-6-Naphthalenesulfonates. *J. Am. Chem. Soc.* **1975**, *97*, 2167–2178.
- (27) Dodiuk, H.; Kosower, E. M. Intramolecular Donor-Acceptor Systems. 2. Substituent Effects on the Fluorescence Probes: 6-(N-Arylamino)-2-Naphthalenesulfonamides. *J. Phys. Chem.* **1977**, *81*, 50–54.
- (28) Strähle, H.; Seitz, W.; Güsten, H. Der Substituenteneinfluss Auf Die Fluoreszenz Des 1,3-Diphenyl-2-Pyrazolins. *Z. Naturforsch., B: J. Chem. Sci.* **1976**, *31*, 1248–1255.
- (29) Zhang, X.; Sun, X.-Y.; Wang, C.-J.; Jiang, Y.-B. Substituent Effect on the Dual Fluorescence of Benzanilides and N-Methylbenzanilides in Cyclohexane. Direct Evidence for Intramolecular Charge Transfer. *J. Phys. Chem. A* **2002**, *106*, 5577–5581.
- (30) Cheshmedzhieva, D.; Ivanova, P.; Stoyanov, S.; Tasheva, D.; Dimitrova, M.; Ivanov, I.; Ilieva, S. Experimental and Theoretical Study on the Absorption and Fluorescence Properties of Substituted Aryl Hydrazones of 1,8-Naphthalimide. *Phys. Chem. Chem. Phys.* **2011**, *13*, 18530–18538.
- (31) Gillanders, F.; Giordano, L.; Díaz, S. A.; Jovin, T. M.; Jares-Erijman, E. A. Photoswitchable Fluorescent Diheteroarylethenes: Substituent Effects on Photochromic and Solvatochromic Properties. *Photochem. Photobiol. Sci.* **2014**, *13*, 603–612.
- (32) Nikolov, P.; Fratev, F.; Polansky, O. E. Correlations of the 0–0 Transitions, the Absorption and Fluorescence Maxima with the 6-Hammett Constants. *J. Mol. Struct.* **1984**, *114*, 265–268.
- (33) Han, M. R.; Hirayama, Y.; Hara, M. Fluorescence Enhancement from Self-Assembled Aggregates: Substituent Effects on Self-Assembly of Azobenzenes. *Chem. Mater.* **2006**, *18*, 2784–2786.
- (34) Kosower, E. M.; Kanety, H.; Dodiuk, H.; Hermolin, J. Bimanes. 9. Solvent and Substituent Effects on Intramolecular Charge-Transfer Quenching of the Fluorescence of Syn-1,5-diazabicyclo [3.3.0]-octadienediones (Syn-9,10-Dioxabimanes). *J. Phys. Chem.* **1982**, *86*, 1270–1277.
- (35) Hirauchi, K.; Amano, T. Studies on the Phosphorimetric Determination of Amines with Halonitro Compounds. II. Substituent Effect on the Fluorescence and Phosphorescence of 4'-substituted 4-Nitrodiphenylamines and 2-(Substituted Anilino)-5-Nitropyridines. *Chem. Pharm. Bull.* **1979**, *27*, 1120–1124.
- (36) Harriman, A.; Hosie, R. J. Luminescence of Porphyrins and Metalloporphyrins. Part 4-Fluorescence of Substituted Tetraphenylporphyrins. *J. Chem. Soc., Faraday Trans. 2* **1981**, *77*, 1695–1702.
- (37) Wagner, P. J.; Truman, R. J.; Scaiano, J. C. Substituent Effects on Hydrogen Abstraction by Phenyl Ketone Triplets. *J. Am. Chem. Soc.* **1985**, *107*, 7093–7097.
- (38) Weir, D.; Scaiano, J. C. Substituent Effects on the Lifetime and Fluorescence of Excited Diphenylmethyl Radicals in Solution. *Chem. Phys. Lett.* **1986**, *128*, 156–159.
- (39) Sakamoto, M.; Cai, X.; Hara, M.; Fujitsuka, M.; Majima, T. Significant Effects of Substituents on Substituted Naphthalenes in the Higher Triplet Excited State. *J. Phys. Chem. A* **2005**, *109*, 4657–4661.
- (40) Wang, J.; Burdzinski, G.; Kubicki, J.; Platz, M. S.; Moss, R. A.; Fu, X.; Piotrowski, P.; Myahkostupov, M. Ultrafast Spectroscopic Study of the Photochemistry and Photophysics of Arylhalodiazirines: Direct Observation of Carbene and Zwitterion Formation. *J. Am. Chem. Soc.* **2006**, *128*, 16446–16447.
- (41) Zhang, Y.; Wang, L.; Moss, R. A.; Platz, M. S. Ultrafast Spectroscopy of Arylchlorodiazirines: Hammett Correlations of Excited State Lifetimes. *J. Am. Chem. Soc.* **2009**, *131*, 16652–16653.
- (42) Rode, M. F.; Sobolewski, A. L. Effect of Chemical Substituents on the Energetical Landscape of a Molecular Photoswitch: An Ab Initio Study. *J. Phys. Chem. A* **2010**, *114*, 11879–11889.
- (43) Vetokhina, V.; Nowacki, J.; Pietrzak, M.; Rode, M. F.; Sobolewski, A. L.; Waluk, J.; Herbich, J. 7-Hydroxyquinoline-8-Carbaldehydes. 1. Ground- and Excited-State Long-Range Prototropic Tautomerization. *J. Phys. Chem. A* **2013**, *117*, 9127–9146.
- (44) Jankowska, J.; Rode, M. F.; Sadlej, J.; Sobolewski, A. L. Excited-State Intramolecular Proton Transfer: Photoswitching in Salicylidene Methylamine Derivatives. *ChemPhysChem* **2014**, *15*, 1643–1652.
- (45) Rode, M. F.; Sobolewski, A. L. Effect of Chemical Substitutions on Photo-Switching Properties of 3-Hydroxy-Picolinic Acid Studied by Ab Initio Methods. *J. Chem. Phys.* **2014**, *140*, 084301.
- (46) Baldry, P. J. Substituent Effects and Excited State Reactivity. *J. Chem. Soc., Perkin Trans. 2* **1979**, No. 7, 951–953.
- (47) Baldry, P. J. Photochemistry of Arylbutadienes. Part 2. Preparation and Photochemistry of 1-(Substituted-Aryl)butadienes. A Ground-State Substituent Effect on an Excited-State Reaction. *J. Chem. Soc., Perkin Trans. 2* **1980**, No. 5, 805–808.
- (48) Shim, S. C.; Chung, J.-S.; Ham, H.-S. The New Substituent Constant in the Excited States. *Bull. Korean Chem. Soc.* **1982**, *3*, 13–18.



- (49) Shim, S.-C.; Park, J.-W.; Ham, H.-S.; Chung, J.-S. The New Substituent Constants in the Excited States (II). *Bull. Korean Chem. Soc.* **1983**, *4*, 45–47.
- (50) Cao, C.; Chen, G.; Yin, Z. Excited-State Substituent Constants  $\sigma_{\text{CC}}^{\text{ex}}$  from Substituted Benzenes. *J. Phys. Org. Chem.* **2008**, *21*, 808–815.
- (51) Burawoy, A. Licht-Absorption Und Konstitution, I. Mitteil.: Homöopolare Organische Verbindungen. *Ber. Dtsch. Chem. Ges. B* **1930**, *63*, 3155–3172.
- (52) Chen, G. F.; Cao, C. Z. Effect of Excited-State Substituent Constant on the UV Spectra of 1,4-Disubstituted Benzenes. *Chin. J. Chem. Phys.* **2009**, *22*, 366–370.
- (53) Chen, G.; Cao, C. Substituent Effect on the UV Spectra of *p*-Disubstituted Compounds  $\text{XPh}(\text{CH}=\text{CHPh})_n$  ( $n = 0, 1, 2$ ). *J. Phys. Org. Chem.* **2010**, *23*, 776–782.
- (54) Yuan, H.; Cao, C.-T.; Cao, Z.; Chen, C.-N.; Cao, C. The Influence of the Excited-State Substituent Effect on the Reduction Potentials of Schiff Bases. *J. Phys. Org. Chem.* **2016**, *29*, 145–151.
- (55) Qian, Z.; Chao-Tun, C.; Chen-Zhong, C.; Qian, Z.; Chao-Tun, C.; Chen-Zhong, C. Extension and Application of Excited-State Constants of *meta*-Substituents. *Wuli Huaxue Xuebao* **2016**, *33*, 729–735.
- (56) Schwartz, S. E. The Franck-Condon Principle and the Duration of Electronic Transitions. *J. Chem. Educ.* **1973**, *50*, 608.
- (57) Sadlej-Sosnowska, N.; Kijak, M. Excited State Substituent Constants: To Hammett or Not? *Struct. Chem.* **2012**, *23*, 359–365.
- (58) Sadlej-Sosnowska, N. On the Way to Physical Interpretation of Hammett Constants: How Substituent Active Space Impacts on Acidity and Electron Distribution in *p*-Substituted Benzoic Acid Molecules. *Pol. J. Chem.* **2007**, *81*, 1123–1134.
- (59) Sadlej-Sosnowska, N. Substituent Active Region – a Gate for Communication of Substituent Charge with the Rest of a Molecule: Monosubstituted Benzenes. *Chem. Phys. Lett.* **2007**, *447*, 192–196.
- (60) Sadlej-Sosnowska, N. Molecular Similarity Based on Atomic Electrostatic Potential. *J. Phys. Chem. A* **2007**, *111*, 11134–11140.
- (61) Sadlej-Sosnowska, N. Evolution of Quantum Similarity Measures: How They Perform in Modeling Hammett Constants. *Pol. J. Chem.* **2009**, *83*, 2215–2224.
- (62) Ozimiński, W. P.; Dobrowolski, J.  $\sigma$ - and  $\pi$ -Electron Contributions To the Substituent Effect: Natural Population Analysis. *J. Phys. Org. Chem.* **2009**, *22*, 769–778.
- (63) Mazurek, A.; Dobrowolski, J.  $\sigma$ - and  $\pi$ -Electron Incorporation Effect in  $\sigma$ - and  $\pi$ -Electron Systems: The sEDA(II) and pEDA(II) Descriptors. *J. Org. Chem.* **2012**, *77*, 2608–2618.
- (64) Mazurek, A.; Dobrowolski, J.  $\sigma$ - and  $\pi$ -Electron Incorporation Effect in  $\sigma$ - and  $\pi$ -Electron Systems: The sEDA(=) and pEDA(=) Descriptors of the Double Bonded Substituent Effect. *Org. Biomol. Chem.* **2013**, *11*, 2997.
- (65) Mazurek, A.; Dobrowolski, J.  $\sigma$ - and  $\pi$ -Electron Incorporation Effect of the Ring-Junction Heteroatom. the sEDA(III) and pEDA(III) Descriptors. *J. Phys. Org. Chem.* **2015**, *28*, 290–297.
- (66) Frisch, M. J.; Trucks, G. W.; Schlegel, H. B.; Scuseria, G. E.; Robb, M. A.; Cheeseman, J. R.; Scalmani, G.; Barone, V.; Mennucci, B.; Petersson, G. A.; et al. *Gaussian 09*, revision D.01; Gaussian Inc.: Wallingford, CT, 2013.
- (67) Hohenberg, P.; Kohn, W. Inhomogeneous Electron Gas. *Phys. Rev.* **1964**, *136* (3B), B864–B871.
- (68) Runge, E.; Gross, E. K. U. Density-Functional Theory for Time-Dependent Systems. *Phys. Rev. Lett.* **1984**, *52*, 997–1000.
- (69) Becke, A. D. Density-Functional Thermochemistry. III. The Role of Exact Exchange. *J. Chem. Phys.* **1993**, *98*, 5648.
- (70) Lee, C.; Yang, W.; Parr, R. G. Development of the Colle-Salvetti Correlation-Energy Formula into a Functional of the Electron Density. *Phys. Rev. B: Condens. Matter Mater. Phys.* **1988**, *37*, 785–789.
- (71) Stephens, P. J.; Devlin, F. J.; Chabalowski, C. F.; Frisch, M. J. Ab Initio Calculation of Vibrational Absorption and Circular Dichroism Spectra Using Density Functional Force Fields. *J. Phys. Chem.* **1994**, *98*, 11623–11627.
- (72) Yanai, T.; Tew, D. P.; Handy, N. C. A New Hybrid Exchange–correlation Functional Using the Coulomb-Attenuating Method (CAM-B3LYP). *Chem. Phys. Lett.* **2004**, *393*, 51–57.
- (73) Grimme, S. Semiempirical GGA-Type Density Functional Constructed with a Long-Range Dispersion Correction. *J. Comput. Chem.* **2006**, *27*, 1787–1799.
- (74) Kendall, R. A.; Dunning, T. H.; Harrison, R. J. Electron Affinities of the First-Row Atoms Revisited. Systematic Basis Sets and Wave Functions. *J. Chem. Phys.* **1992**, *96*, 6796–6806.
- (75) Woon, D. E.; Dunning, T. H. Gaussian Basis Sets for Use in Correlated Molecular Calculations. III. The Atoms Aluminum through Argon. *J. Chem. Phys.* **1993**, *98*, 1358–1371.
- (76) Grimme, S.; Antony, J.; Ehrlich, S.; Krieg, H. A Consistent and Accurate *Ab Initio* Parametrization of Density Functional Dispersion Correction (DFT-D) for the 94 Elements H–Pu. *J. Chem. Phys.* **2010**, *132*, 154104.
- (77) Glendening, E. D.; Landis, C. R.; Weinhold, F. Natural Bond Orbital Methods. *Wiley Interdiscip. Rev. Comput. Mol. Sci.* **2012**, *2*, 1–42.
- (78) *SigmaPlot 13*; Systat Software, 2017.
- (79) Cvitaš, T.; Hollas, J. M.; Kirby, G. H. Interpretation of Rotational Constants of the First Singlet Excited State of Substituted Benzenes in Terms of Molecular Geometry. *Mol. Phys.* **1970**, *19*, 305–316.
- (80) Gilman, H.; Breuer, F. The Mechanism of Reaction of Phenyl-Sodium and Phenyl-Lithium with Phenyl Isothiocyanate. *J. Am. Chem. Soc.* **1933**, *55*, 1262–1264.
- (81) Kojima, T.; Hiraoka, S. Mesityllithium and *p*-(Dimethylamino)-phenyllithium for the Selective Alternate Trilithiation of the Hexaphenylbenzene Framework. *Chem. Commun.* **2014**, *50*, 10420–10423.
- (82) Fukuda, R.; Ehara, M. Electronic Excited States and Electronic Spectra of Biphenyl: A Study Using Many-Body Wavefunction Methods and Density Functional Theories. *Phys. Chem. Chem. Phys.* **2013**, *15*, 17426–17434.
- (83) Mewes, J.-M.; Jovanović, V.; Marian, C. M.; Dreuw, A. On the Molecular Mechanism of Non-Radiative Decay of Nitrobenzene and the Unforeseen Challenges This Simple Molecule Holds for Electronic Structure Theory. *Phys. Chem. Chem. Phys.* **2014**, *16*, 12393–12406.
- (84) Giussani, A.; Worth, G. A. Insights into the Complex Photophysics and Photochemistry of the Simplest Nitroaromatic Compound: A CASPT2//CASSCF Study on Nitrobenzene. *J. Chem. Theory Comput.* **2017**, *13*, 2777–2788.
- (85) Arenas, J. F.; Otero, J. C.; Peláez, D.; Soto, J. CASPT2 Study of the Decomposition of Nitrosomethane and Its Tautomerization Reactions in the Ground and Low-Lying Excited States. *J. Org. Chem.* **2006**, *71*, 983–991.
- (86) Alam, M. M.; Ito, O. Photochemistry of Nitrobenzenethiol. Selective Generation of the Thio Radical and Thione Triplet State as a Function of Solvent Polarity. *J. Org. Chem.* **1999**, *64*, 1285–1290.
- (87) Riyad, Y. M.; Naumov, S.; Hermann, R.; Brede, O. Deactivation of the First Excited Singlet State of Thiophenols. *Phys. Chem. Chem. Phys.* **2006**, *8*, 1697–1706.
- (88) Pietraperzia, G.; Becucci, M.; Pace, I. D.; López-Tocón, I.; Castellucci, E. Rotationally Resolved Electronic Spectroscopy of Aniline Excited Vibronic Levels. *Chem. Phys. Lett.* **2001**, *335*, 195–200.
- (89) Sinha, H. K.; Yates, K. On the Ground and Excited State Dipole Moments of Planar vs. Twisted Nitroaniline Analogues. *Can. J. Chem.* **1991**, *69*, 550–557.
- (90) Mazurek, A. Electron Donor Acceptor Descriptors of the Single and Double Bonded Substituent and Heteroatom Incorporation Effects. A Review. *Acta Polonicae Pharmaceutica. Drug Research* **2016**, *73*, 269–283.
- (91) Hammett, L. P. Some Relations between Reaction Rates and Equilibrium Constants. *Chem. Rev.* **1935**, *17*, 125–136.
- (92) Hammett, L. P. The Effect of Structure upon the Reactions of Organic Compounds. Benzene Derivatives. *J. Am. Chem. Soc.* **1937**, *59*, 96–103.



- (93) Jaffé, H. H. A Reëxamination of the Hammett Equation. *Chem. Rev.* **1953**, *53*, 191–261.
- (94) Hęclik, K.; Dębska, B.; Dobrowolski, J. Cz On the Non-Additivity of the Substituent Effect in Ortho-, Meta- and Para-Homo-Disubstituted Benzenes. *RSC Adv.* **2014**, *4*, 17337–17346.
- (95) Hęclik, K.; Dobrowolski, J. Cz On the Nonadditivity of the Substituent Effect in Homo-Disubstituted Pyridines. *J. Phys. Org. Chem.* **2017**, *30*, e3656.
- (96) Hoffmann, R.; Woodward, R. B. Selection Rules for Concerted Cycloaddition Reactions. *J. Am. Chem. Soc.* **1965**, *87*, 2046–2048.
- (97) Fukui, K. Role of Frontier Orbitals in Chemical Reactions. *Science* **1982**, *218*, 747–754.
- (98) Jensen, W. B. The Lewis Acid-Base Definitions: A Status Report. *Chem. Rev.* **1978**, *78*, 1–22.
- (99) Baranoff, E.; Curchod, B. F. E.; Monti, F.; Steimer, F.; Accorsi, G.; Tavernelli, I.; Rothlisberger, U.; Scopelliti, R.; Grätzel, M.; Nazeeruddin, M. K. Influence of Halogen Atoms on a Homologous Series of Bis-Cyclometalated Iridium(III) Complexes. *Inorg. Chem.* **2012**, *51*, 799–811.
- (100) Dou, L.; Liu, Y.; Hong, Z.; Li, G.; Yang, Y. Low-Bandgap Near-IR Conjugated Polymers/Molecules for Organic Electronics. *Chem. Rev.* **2015**, *115*, 12633–12665.
- (101) Koopmans, T. Über Die Zuordnung von Wellenfunktionen Und Eigenwerten Zu Den Einzelnen Elektronen Eines Atoms. *Physica* **1934**, *1*, 104–113.
- (102) Helgaker, T.; Jorgensen, J.; Olsen, J. *Molecular Electronic Structure Theory*; Wiley, 2000.
- (103) Baerends, E. J.; Gritsenko, O. V.; van Meer, R. The Kohn–Sham Gap, the Fundamental Gap and the Optical Gap: The Physical Meaning of Occupied and Virtual Kohn–Sham Orbital Energies. *Phys. Chem. Chem. Phys.* **2013**, *15*, 16408–16425.
- (104) van Meer, R.; Gritsenko, O. V.; Baerends, E. J. Physical Meaning of Virtual Kohn–Sham Orbitals and Orbital Energies: An Ideal Basis for the Description of Molecular Excitations. *J. Chem. Theory Comput.* **2014**, *10*, 4432–4441.
- (105) Levy, M.; Nagy, Á. Excited-State Koopmans Theorem for Ensembles. *Phys. Rev. A: At., Mol., Opt. Phys.* **1999**, *59*, 1687–1689.
- (106) Nagy, Á.; Adachi, H. Total Energy versus One-Electron Energy Differences in the Excited-State Density Functional Theory. *J. Phys. B: At., Mol. Opt. Phys.* **2000**, *33*, L585–L589.
- (107) Ghosh, R.; Nandi, A.; Palit, D. K. Solvent Sensitive Intramolecular Charge Transfer Dynamics in the Excited States of 4-N,N-Dimethylamino-4'-Nitrobiphenyl. *Phys. Chem. Chem. Phys.* **2016**, *18*, 7661–7671.
- (108) Pearson, R. G. Absolute Electronegativity and Hardness Correlated with Molecular Orbital Theory (Polarizability/visible-Ultraviolet Spectra/ionization Potential/electron Affinity). *Proc. Natl. Acad. Sci. U. S. A.* **1986**, *83*, 8440–8441.